Available online at www.sciencedirect.com
ScienceDirect
Journal of Computational Physics 218 (2006) 549–571
JOURNAL OF COMPUTATIONAL PHYSICS
www.elsevier.com/locate/jcp

2D nearly orthogonal mesh generation with controls on distortion function

Yaoxin Zhang *,[1], Yafei Jia [2], Sam S.Y. Wang [3]

National Center for Computational Hydroscience and Engineering, The University of Mississippi, Carrier Hall, Room 102, P.O. Box 1500, University, Oxford, MS 38677, United States

Received 14 September 2005; received in revised form 22 February 2006; accepted 23 February 2006
Available online 27 April 2006

Abstract

A method to control the distortion function of the Ryskin and Leal (RL) orthogonal mesh generation system is presented. The proposed method considers the effects from not only the local orthogonal condition but also the local smoothness condition (the geometry and the mesh size) on the distortion function. The distortion function is determined by both the scale factors and the averaged scale factors of the constant mesh lines. Two adjustable parameters are used to control the local balance of the orthogonality and the smoothness. The proposed method is successfully applied to several benchmark examples and the natural river channels with complex geometries.

Keywords: Mesh generation; Distortion function; Scale factor

1. Introduction

It is generally accepted that regardless of the discretization method, the quality of a computational mesh, usually characterized by the orthogonality and the smoothness, has significant influences on the solutions of the non-linear partial differential equations (PDE). Although extensive research (for examples, see [1–14]) has been made on high quality mesh generation, the generation of orthogonal mapping with adequate smoothness in geometrically complex domains still remains a challenge.

Many methodologies and techniques have been proposed for orthogonal mesh generation since late 1970s (see [1–12,14]). Conformal mapping is the most well-known orthogonal mapping. It is simple, efficient and easy to use. However, because it requires equal scale factors in all directions, the conformal mapping may cause folded meshes at the concave boundaries. Ryskin and Leal [10] proposed a covariant Laplace equation

* Corresponding author. Tel.: +1 662 915 3960; fax: +1 662 915 7796.
E-mail address: yzhang@ncche.olemiss.edu (Y. Zhang).
[1] Post-Doctoral Research Associate.
[2] Research Associate Professor and Assistant Director for Basic Research of National Center for Computational Hydroscience and Engineering.
[3] F.A.P Barnard Distinguished Professor and Director of National Center for Computational Hydroscience and Engineering.

0021-9991/$ - see front matter
doi:10.1016/j.jcp.2006.02.023

system for orthogonal mapping (often referred as RL system). The RL system has been the objective of many researchers (see [1–6,8,11,14]). The focus of these researches was the determination of the distortion function f, which generally cannot be prescribed arbitrarily. Eça [5] classified three different treatments of the distortion function: (1) calculate f from its definition at the boundaries and then obtain the values in the domain by interpolation or by solving a Laplace equation (see [10,11]); (2) specify a class of admissible functions for f based on the quasi-conformal mapping theory to guarantee a unique solution (see [3,4]); and (3) calculate f from its definition for the whole domain (see [1,2,5]).

According to its definition, the distribution of the distortion function f actually describes the mesh density distribution. In the first two methods, the distortion function f is controlled algebraically or numerically, while in the third method there are no controls on the distortion function f. Therefore, the above three methods can be simply categorized into two groups: methods with controls on distortion function and methods without controls on distortion function. For methods without controls on the distortion function f, the mesh density or aspect ratio is controlled only by the local orthogonal condition and consequently its distribution in the whole domain is not predicable. It is already pointed out by Eça [5], Akcelik et al. [1] and Zhang et al. [14] that the RL system may cause serious mesh distortions or overlapping in complex geometries when using the ''weak constraint'' method with the specified boundary point distribution for all boundaries.

In this paper, a new method of formulating the distortion function is proposed. In addition to the local scale factors, the globally averaged scale factors of the constant mesh lines are also used to evaluate the distortion function f. Local balance of the orthogonality and the smoothness is controlled by two adjustable empirical parameters which are evaluated automatically based on the deviation from the local smoothness condition. Several examples and applications are used to test and illustrate the proposed method. It is demonstrated that this method is effective and easy to use.

2. Elliptic mesh generation systems

The RL system proposed by Ryskin and Leal [10] and the conformal mapping system are two classical elliptic orthogonal mapping systems. The former, a covariant Laplace equation system, can be easily derived in a way analogue to the Laplace equations for stream function and velocity potential function. In the RL system, the orthogonal mapping between the physical coordinates ($x^i(\equiv x, y)$, $i = 1, 2$) and the computational coordinates ($\xi^i(\equiv \xi, \eta)$, $i = 1, 2$) can be described using the following covariant equations:

$$\frac{\partial}{\partial \xi}\left(f\frac{\partial x}{\partial \xi}\right) + \frac{\partial}{\partial \eta}\left(\frac{1}{f}\frac{\partial x}{\partial \eta}\right) = 0 \tag{1a}$$

$$\frac{\partial}{\partial \xi}\left(f\frac{\partial y}{\partial \xi}\right) + \frac{\partial}{\partial \eta}\left(\frac{1}{f}\frac{\partial y}{\partial \eta}\right) = 0 \tag{1b}$$

where the distortion factor f (also called aspect ratio) is defined as the ratio of the scale factors in ξ and η directions:

$$f = \frac{h_\eta}{h_\xi} = \left(\frac{x_\eta^2 + y_\eta^2}{x_\xi^2 + y_\xi^2}\right)^{1/2} \tag{2a}$$

$$h_\xi = g_{11}^{1/2}, \quad h_\eta = g_{22}^{1/2} \tag{2b}$$

where $x_\xi = \partial x/\partial \xi$ and so forth.

In Eq. (2), the metric tensor g_{ij} represents the physical features of a computational mesh and it is defined as follows:

$$g = \begin{vmatrix} (x_\xi^2 + y_\xi^2) & (x_\xi x_\eta + y_\xi y_\eta) \\ (x_\xi x_\eta + y_\xi y_\eta) & (x_\eta^2 + y_\eta^2) \end{vmatrix} \tag{3}$$

Using the central difference scheme to discretize Eq. (1) at one typical mesh node (i, j), one can obtain:

$$F_{i,j}x_{i,j} = f_{i+1/2,j}x_{i+1,j} + f_{i-1/2,j}x_{i-1,j} + \frac{1}{f_{i,j+1/2}}x_{i,j+1} + \frac{1}{f_{i,j-1/2}}x_{i,j-1} \tag{4a}$$

$$F_{i,j}y_{i,j} = f_{i+1/2,j}y_{i+1,j} + f_{i-1/2,j}y_{i-1,j} + \frac{1}{f_{i,j+1/2}}y_{i,j+1} + \frac{1}{f_{i,j-1/2}}y_{i,j-1} \tag{4b}$$

where $F_{i,j} = f_{i+1/2,j} + f_{i-1/2,j} + \frac{1}{f_{i,j+1/2}} + \frac{1}{f_{i,j-1/2}}$.

The conformal mapping system is well known with equal scale factors in all directions. That is,

$$h_\xi = h_\eta, \quad f = \frac{h_\eta}{h_\xi} = 1 \tag{5}$$

Eq. (5) is called the *absolute smoothness condition*. Substitution of Eq. (5) into Eq. (1) leads to the following conformal mapping system:

$$\frac{\partial^2 x}{\partial \xi^2} + \frac{\partial^2 x}{\partial \eta^2} = 0 \tag{6a}$$

$$\frac{\partial^2 y}{\partial \xi^2} + \frac{\partial^2 y}{\partial \eta^2} = 0 \tag{6b}$$

The conformal mapping system defined by Eq. (6) can be considered as a special case of the RL system with $f = 1$ satisfied in the whole domain.

To resolve the mesh distortion and overlapping problems, Zhang et al. [14] proposed another method to control the distortion function. The distortion function is first calculated from its definition in the entire domain and then a contribution factor which is evaluated by the local scale factor is used to confine the effects of the distortion function. Their method can be described as follows:

$$f^* = f \cdot h_\xi^\alpha \text{ (in } \xi \text{ direction)} \tag{7a}$$

$$\left(\frac{1}{f}\right)^* = \frac{1}{f} \cdot h_\eta^\alpha \text{ (in } \eta \text{ direction)} \tag{7b}$$

where f is the distortion function calculated from its definition, f^* and $\left(\frac{1}{f}\right)^*$ are the actual distortion function during the computation, h_ξ^α and h_η^α are the so-called contribution factors, and α is an adjustable exponential parameter.

3. Current study

The RL system emphasizes on the orthogonality but ignores the smoothness, while the conformal mapping is too strict in the smoothness. To improve their disadvantages, a new method is proposed in the current study.

3.1. Averaged scale factors

Let us consider a simple rectangular domain with a width of W (ξ direction), a height of H(η direction), and a mesh size of $N \times M$. A uniform nodal distribution is assumed along all the boundaries. For this simple domain, the constraint of the local orthogonal condition on the distortion function is already excluded, and the same resulting mesh can be obtained by the RL and conformal mapping generation systems. For internal mesh nodes, the final distortion functions can be obtained as follows:

$$f = \frac{h_\eta}{h_\xi} = \frac{H/(M-1)}{W/(N-1)} \tag{8}$$

where the local scale factors h_ξ and h_η are actually equal to the averaged scale factors.

Defined by the ratio of the scale factors in two different directions, the distortion function is obviously related to both the geometry of the domain and the mesh size. As for geometrically complex domains, the final distortion function of the resulting mesh is not predicable due to the fact that it is controlled only by the local orthogonal condition. For the conformal system, the strict *absolute smoothness condition* ($f = 1$) is difficult to

be satisfied for the whole domain, although this condition is enforced in the derivation of the generation equations.

The current study proposes that the averaged scale factors along constant mesh lines be used to evaluate the distortion function. For one typical mesh node (i, j), one can obtain:

$$\overline{f_{i,j}} = \frac{(\overline{h_\eta})_j}{(\overline{h_\xi})_i} \tag{9}$$

$$(\overline{h_\xi})_i = \frac{1}{N_j - 2} \sum_{j=2}^{N_j - 1} (h_\xi)_{i,j} \tag{10a}$$

$$(\overline{h_\eta})_j = \frac{1}{N_i - 2} \sum_{i=2}^{N_i - 1} (h_\eta)_{i,j} \tag{10b}$$

where $\overline{f_{i,j}}$ is the local averaged distortion function, $(\overline{h_\xi})_i$ and $(\overline{h_\eta})_j$ are the global averaged scale factors at $\xi = i$ line and at $\eta = j$ line, respectively; and, N_i and N_j are the total number of mesh lines in ξ and η directions.

Eq. (9) implies that the following smoothness conditions are enforced:

$$(h_\xi)_{i,j} = (\overline{h_\xi})_i \tag{11a}$$

$$(h_\eta)_{i,j} = (\overline{h_\eta})_j \tag{11b}$$

Correspondingly, Eqs. (11a) and (11b) are called the *relative smoothness conditions* in ξ and η directions, respectively. Compared with its original definition (Eq. (2)), the distortion function evaluated by Eq. (9) considers both the global effects of the geometry and the mesh size. Consequently, the relaxed local orthogonal condition results in less orthogonal but smoother (nearly orthogonal) meshes. As demonstrated in [14], a certain degree of compromise of the orthogonality for improving smoothness is necessary and worthwhile for geometrically complex domains, in which it is difficult to generate an acceptable mesh without mesh distortion and overlapping using the RL system. Compared with the constant distortion function (*absolute smoothness condition*) enforced in the conformal mapping system, Eq. (9) replaces the strict smoothness condition with the *relative smoothness conditions*.

Eq. (9) controls the scale factors to enforce the local smoothness in both directions. In cases only one of the directions needs to be controlled, one can obtain the following two alternatives which control the scale factors only in ξ direction or η direction, respectively:

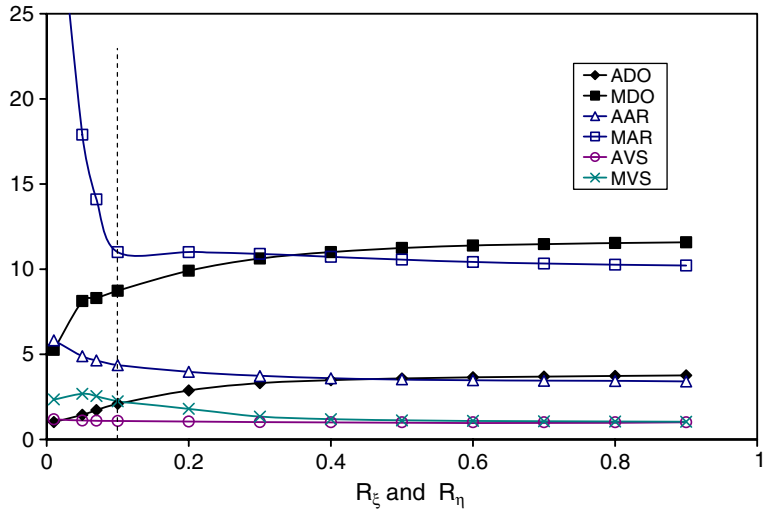

Fig. 1. Effects of r_ξ and r_η on mesh quality.

$$\text{To control the } \xi \text{ direction}: \quad \overline{f_{i,j}} = \frac{(h_\eta)_{i,j}}{(\overline{h_\xi})_i} \tag{12}$$

$$\text{To control the } \eta \text{ direction}: \quad \overline{f_{i,j}} = \frac{(\overline{h_\eta})_j}{(h_\xi)_{i,j}} \tag{13}$$

3.2. Balance of orthogonality and smoothness

It has been shown the averaged scale factors $(\overline{h_\xi})_i$ and $(\overline{h_\eta})_j$ defined by Eq. (10) can characterize the local smoothness; similarly the local scale factors defined by Eq. (2b) can characterize the local orthogonality. Therefore, the local balance of the orthogonality and the smoothness can be controlled through the ratio between the averaged scale factors and the local scale factors. This inspires an immediate extension of Eqs. (9), (12) and (13):

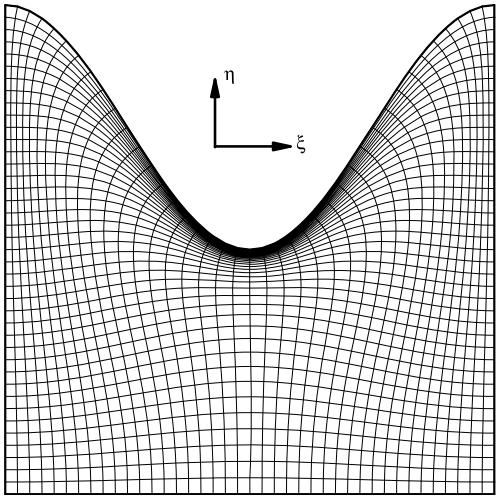

(A1) RL with $r_\xi = 0$ and $r_\eta = 0$.

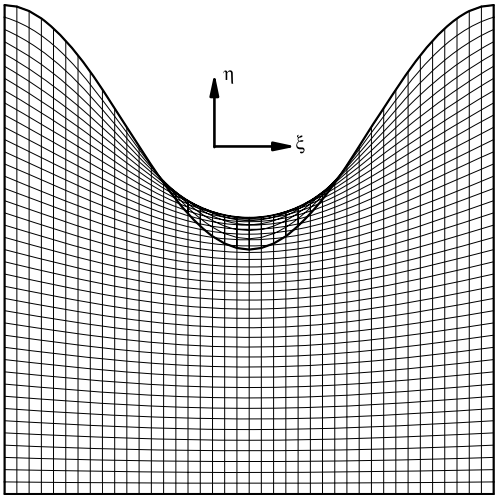

(A2) Conformal mapping.

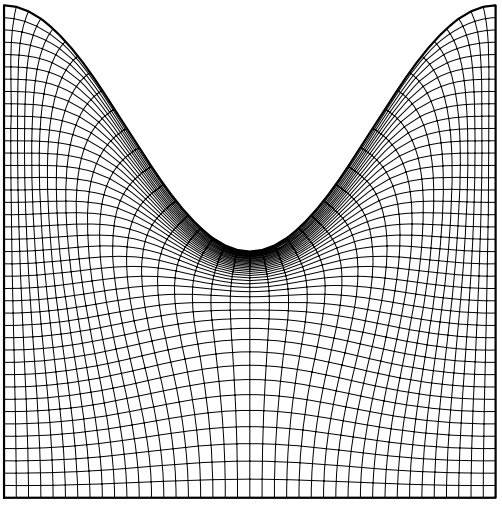

(A3) RL with contribution factors.

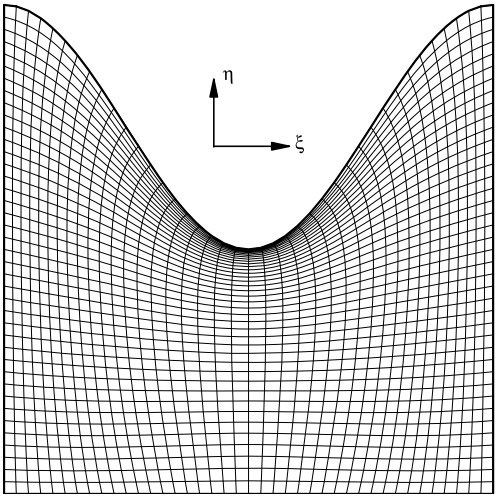

(A4) RL with $r_\xi = 0.5$ and $r_\eta = 0.5$.

Fig. 2. Meshes in domain A.

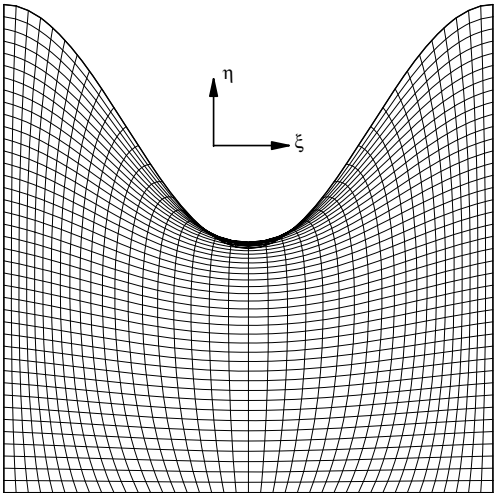

(A5) RL with $r_\xi = 1$ and $r_\eta = 1$.

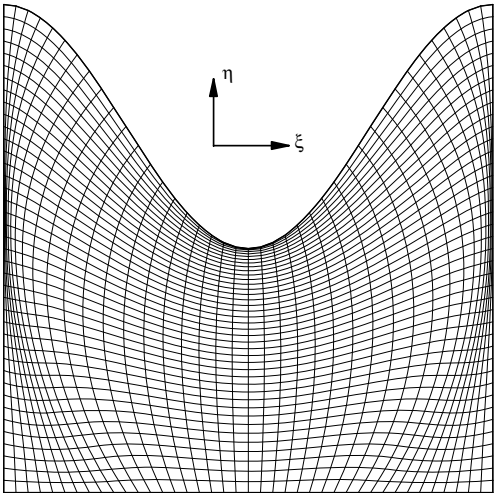

(A6) RL with $r_\xi = 0$ and $r_\eta = 1$.

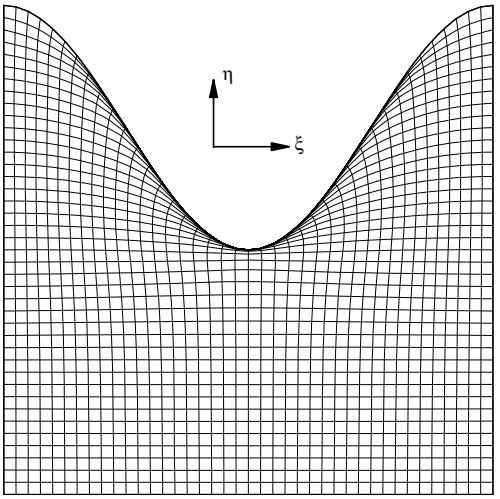

(A7) RL with $r_\xi = 1$ and $r_\eta = 0$.

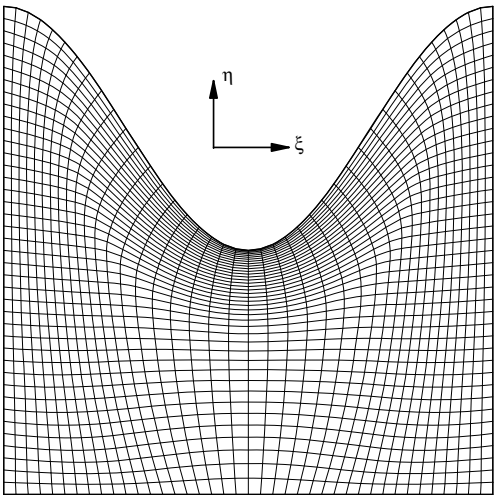

(A8) RL with r_ξ and r_η evaluated by Eq. (15).

Fig. 2 (*continued*)

$$\overline{f_{i,j}} = \frac{(\overline{h_\eta})_j \cdot r_\eta + (h_\eta)_{i,j} \cdot (1 - r_\eta)}{(\overline{h_\xi})_i \cdot r_\xi + (h_\xi)_{i,j} \cdot (1 - r_\xi)} \tag{14}$$

where r_η and r_ξ are two adjustable parameters within the range of [0, 1] for controlling the ratio between the averaged scale factors and the local scale factors.

With the two empirical parameters r_η and r_ξ, Eq. (14) is more capable and flexible than its predecessors – Eqs. (9), (12) and (13). Eqs. (2), (9), (12) and (13) can be obtained from Eq. (14) by specifying different values of these two parameters. With both parameters set to be zero, Eq. (2) – the original definition of the distortion function can be obtained; to obtain Eq. (9), both of them should be equal to 1; and, if either one is equal to 1 and another is equal to 0, Eq. (12) or (13) can be derived. In case the *relative smoothness conditions*, the local scale factors are equal to the averaged scale factors, are satisfied (not enforced), these two parameters will vanish automatically.

Obviously, the parameters r_η and r_ξ can be user-specified. It can be either constant or have a specified distribution through the whole domain. Although the manual evaluation is flexible, the evaluation process may be tedious in order to obtain a good resulting mesh. In the current study, an automatic evaluation mechanism is established for these two empirical parameters.

$$[r_\xi]_{i,j} = \frac{|(h_\xi)_{i,j} - (\overline{h_\xi})_i|}{(h_\xi)_{i,j} + (\overline{h_\xi})_i} \tag{15a}$$

$$[r_\eta]_{i,j} = \frac{|(h_\eta)_{i,j} - (\overline{h_\eta})_j|}{(h_\eta)_{i,j} + (\overline{h_\eta})_j} \tag{15b}$$

In Eq. (15), the difference between the local scale factor and the averaged scale factor measures the deviation from the local *relative smoothness condition*. The parameters r_η and r_ξ, evaluated by the ratio of the difference and the sum of the local scale factors and the averaged scale factor in the corresponding directions,

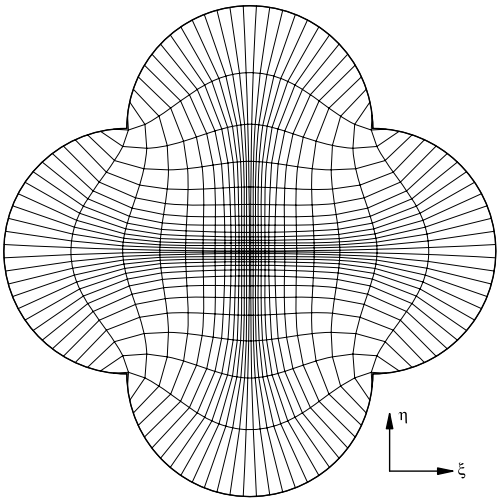

(B1) RL with $r_\xi = 0$ and $r_\eta = 0$.

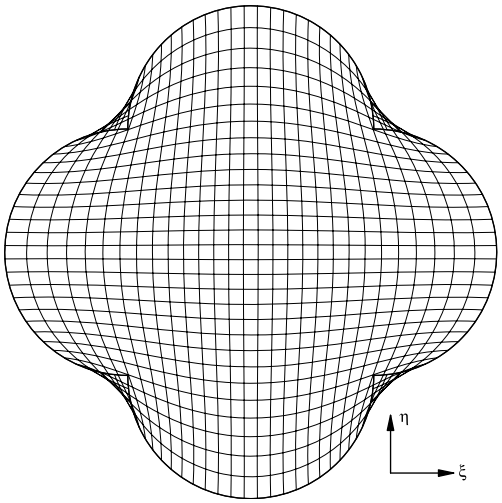

(B2) Conformal mapping.

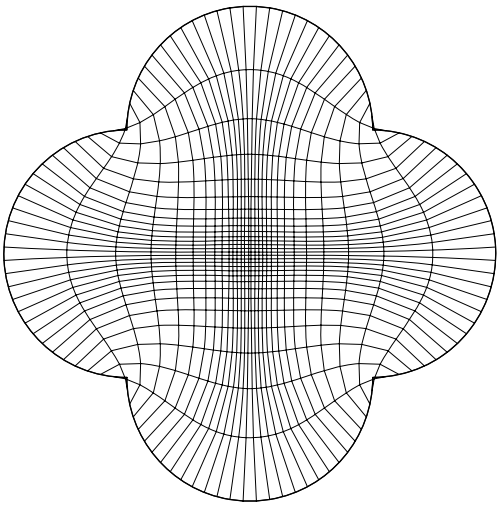

(B3) RL with contribution factors.

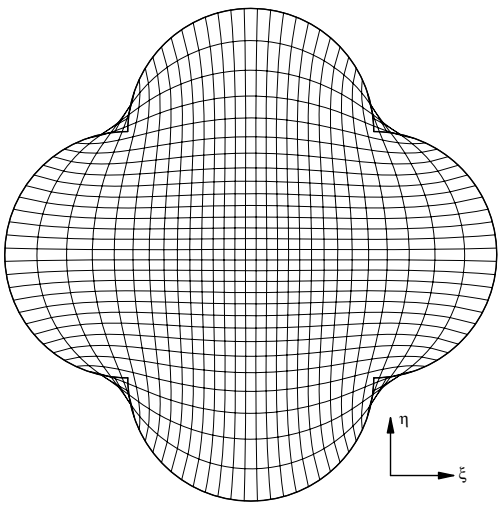

(B4) RL with $r_\xi = 0.5$ and $r_\eta = 0.5$.

Fig. 3. Meshes in domain B.

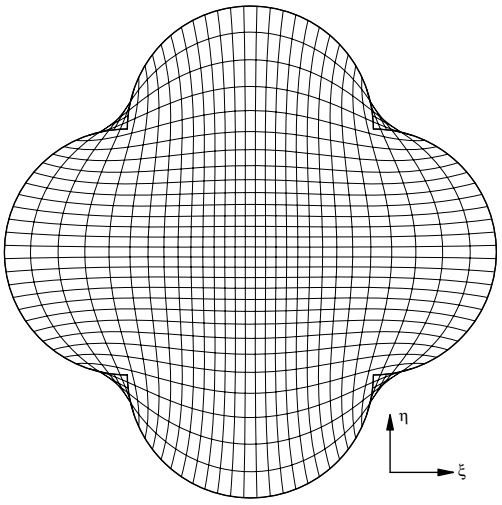

(B5) RL with $r_\xi = 1$ and $r_\eta = 1$.

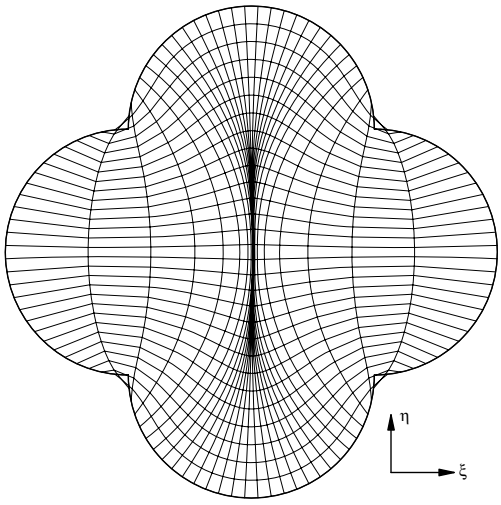

(B6) RL with $r_\xi = 0$ and $r_\eta = 1$.

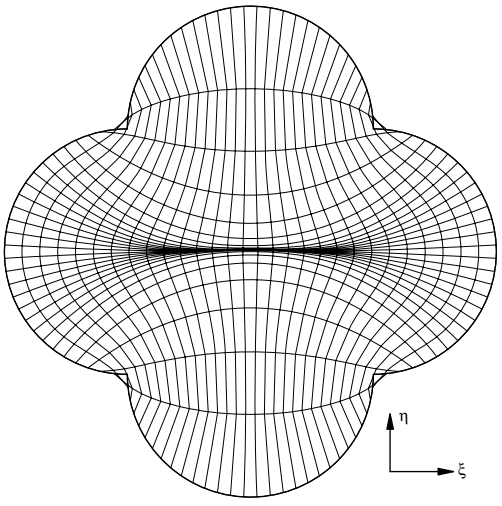

(B7) RL with $r_\xi = 1$ and $r_\eta = 0$.

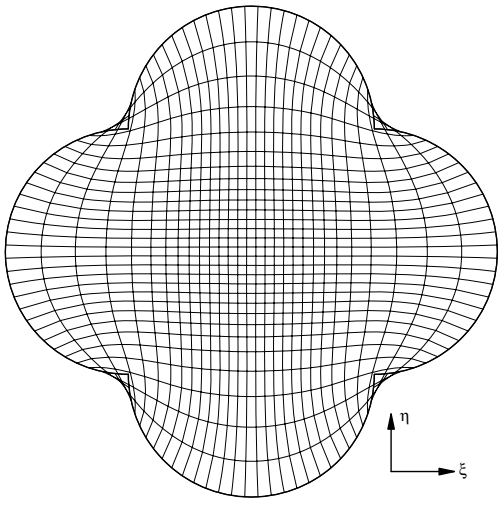

(B8) RL with r_ξ and r_η evaluated by Eq. (15).

Fig. 3 (*continued*)

are actually the indicators of the local *relative smoothness condition*. Smaller values of these parameters indicate improved local smoothness and reduced effects of the average scale factors and vice versa. The zero value of these parameters implies that the local *relative smoothness conditions* are satisfied. With this adjustment mechanism, a global balance between the orthogonality and the smoothness can be reached.

3.3. Comparisons with previous studies

As stated previously, Akcelik et al. [1] (RL with source terms) and Zhang et al. [14] (RL with contribution factors) modified the original RL system in order to resolve the mesh distortion and overlapping problems in geometrically complex domains when using "weak constraint" method [10]. The former introduced the inhomogeneous source terms with a parameter to tune their intensities, while the latter introduced a contribution factor to confine the uncontrolled growth of the distortion function. An exponential parameter was used to adjust the effects of the contribution factors.

Table 1
Evaluation of meshes in domains A and B

Domain	Case	Size	ADO	MDO	AAR	MAR	AVS	MVS	r_ξ	r_η	α
A	A1	41×41	0.07	0.62	4.86	33.9	1.07	1.25	0	0	–
	A2	41×41	3.18	11.62	2.98	411.3	1.15	20.7	–	–	–
	A3	41×41	0.15	0.72	3.57	13.7	1.04	1.25	–	–	0.01
	A4	41×41	3.10	7.27	2.39	30.08	1.04	1.46	0.5	0.5	–
	A5	41×41	3.74	14.46	2.34	68.38	1.04	3.45	1	1	–
	A6	41×41	3.77	6.76	2.83	16.34	1.09	2.58	0	1	–
	A7	41×41	1.32	6.16	2545	70,129	1.25	3.91	1	0	–
	A8	41×41	2.16	4.76	2.47	12.1	1.05	1.36	–	–	–
B	B1	30×30	0.07	4.28	4.22	13.0	1.25	1.42	0	0	–
	B2	30×30	4.63	14.6	1.19	1.61	1.03	1.07	–	–	–
	B3	30×30	0.19	8.0	3.31	9.4	1.22	1.39	–	–	0.01
	B4	30×30	2.65	14.45	1.51	2.63	1.08	1.18	0.5	0.5	–
	B5	30×30	2.82	14.38	1.53	2.44	1.05	1.12	1	1	–
	B6	30×30	0.72	14.26	31.4	816.	1.39	3.09	0	1	–
	B7	30×30	0.72	14.26	31.4	816.	1.39	3.09	1	0	–
	B8	30×30	1.84	14.22	1.74	3.36	1.10	1.31	–	–	–

The following points differentiate the above two methods and the present method:

(1) The RL with source terms is a Poisson equation system, while the RL with contribution factors and the present method remain a Laplace equation system.
(2) In the cases of RL with source terms and the RL with contribution factors, the distortion function is calculated from its definition – Eq. (2), while in the present method the distortion function is evaluated by a composite function constructed with the scale factors and the averaged scale factors – Eq. (14).
(3) The RL with source terms does not have controls on the distortion function, but the RL with contribution factors and the present method do.
(4) The two parameters in the present method are used to control the local balance of orthogonality and smoothness, while the parameters in the other two methods are used to control the intensities of the source terms and the contribution factors, respectively.
(5) An automatic evaluation mechanism has been established for the two parameters in the present method, while the parameters in the other two methods must be user-specified.
(6) Compared to the parameters in the RL with contribution factors and the present method, the parameter in the RL with source terms is unbounded, which makes it difficult to use.

Since the RL with contribution factors and the present method fall into the same category: methods with controls on the distortion function, further comparisons will be conducted for them using examples.

4. Solution process

The RL system defined by Eq. (1) is highly non-linear. In the current study, an iterative method similar to that of [5] is used to solve the linear equation (4). The iterative algorithm is simply listed as follows:

1. Define the boundaries of a computational domain and use an algebraic method to generate an initial mesh.
2. Evaluate the parameters r_η and r_ξ manually or using Eq. (15).
3. Calculate the distortion function f from Eq. (14).
4. Solve Eq. (4) with fixed f obtained from step 3.
5. Update the mesh and check if the convergence condition is satisfied. If not, repeat steps from 2 through 5.

Two convergence criterions are used and the satisfaction of either one will stop the computation. The first one is the maximum difference between the grid coordinates in consecutive steps and the second one is the maximum relative difference of the distortion function f between consecutive iterations. They are defined as follows:

$$\max\left(\sqrt{(x_{i,j}^n - x_{i,j}^{n-1})^2 + (y_{i,j}^n - y_{i,j}^{n-1})^2}\right) < 10^{-6} \tag{16}$$

$$\max\left(\frac{f^n - f^{n-1}}{f^n}\right) < 10^{-6} \tag{17}$$

where n is the iteration number.

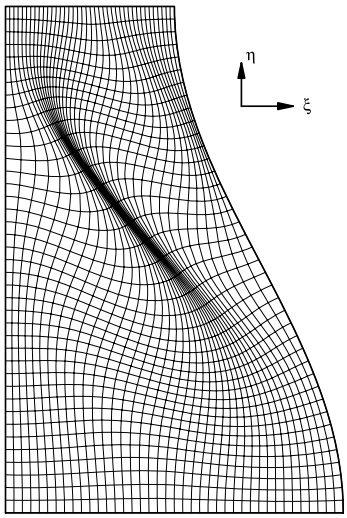

(C1) RL with $r_\xi = 0$ and $r_\eta = 0$.

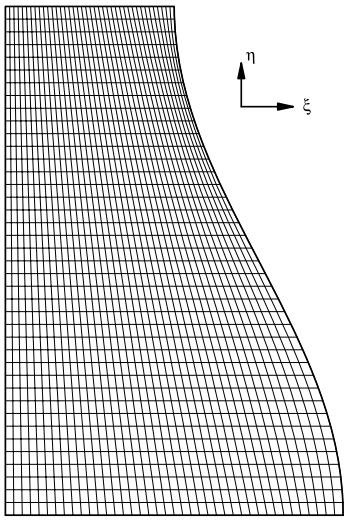

(C2) Conformal mapping.

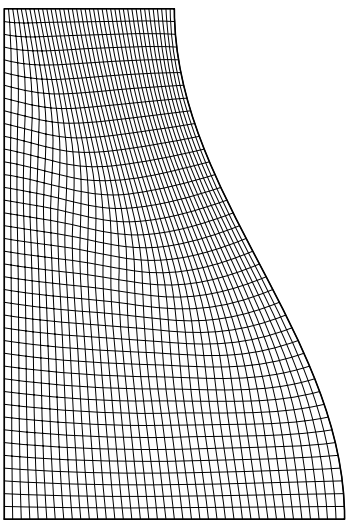

(C3) RL with contribution factors.

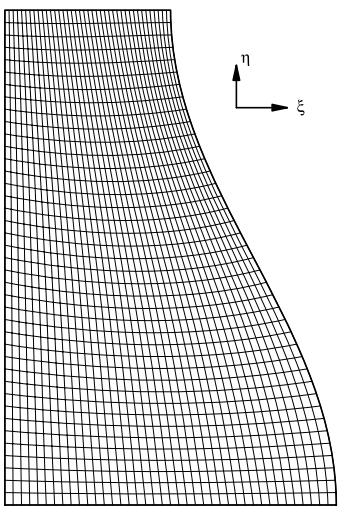

(C4) RL with $r_\xi = 0.5$ and $r_\eta = 0.5$.

Fig. 4. Meshes in domain C.

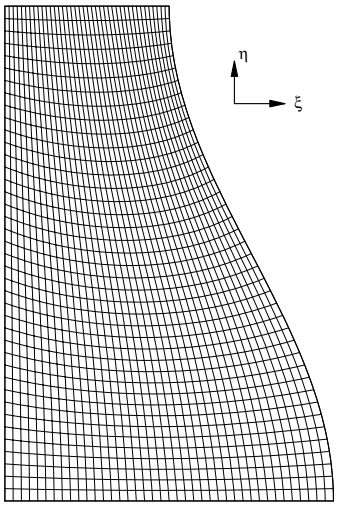

(C5) RL with $r_\xi = 1$ and $r_\eta = 1$.

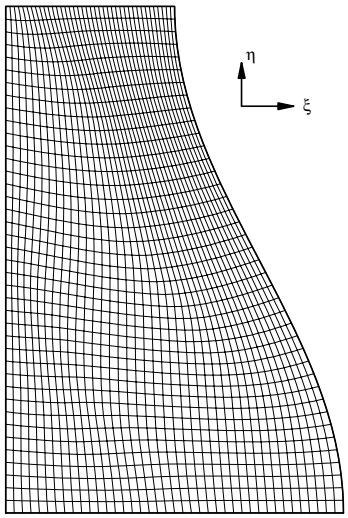

(C6) RL with $r_\xi = 0$ and $r_\eta = 1$.

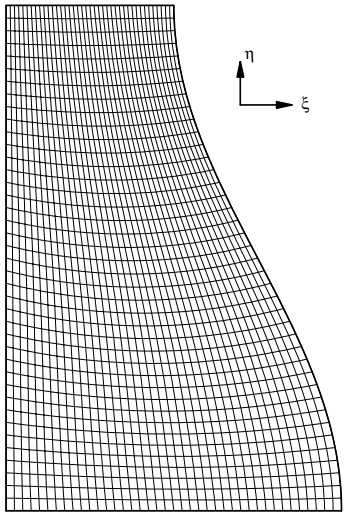

(C7) RL with $r_\xi = 1$ and $r_\eta = 0$.

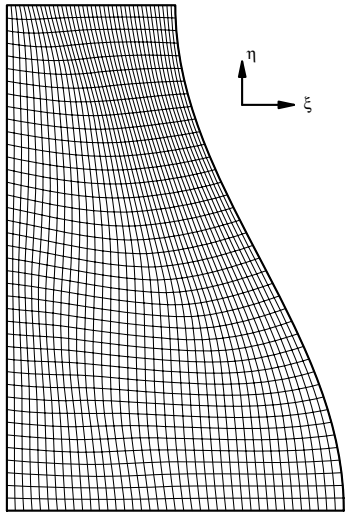

(C8) RL with r_ξ and r_η evaluated by Eq. (15).

Fig. 4 (*continued*)

5. Boundary conditions

The boundary conditions have significant influences on the resulting meshes. Actually, selecting the appropriate boundary conditions to guarantee a unique solution of the RL system remains a big concern (see [6,8,10]). Two types of boundary conditions are available: the Dirichlet boundary condition with the fixed specified nodal distribution along the boundaries, and the Dirichlet-Neumann boundary condition (also called sliding boundary condition) which allows the mesh nodes slide along the boundaries (Dirichlet) to satisfy the Neumann condition.

In the present study, only the Dirichlet boundary conditions are used for all the boundaries to test the proposed method. There is no theoretical proof that the application of the Dirchlet boundary condition would guarantee a unique solution. However, as demonstrated numerically by Eça [5] and Zhang et al. [14], a converged solution of the RL system is possible with this type of the boundary condition.

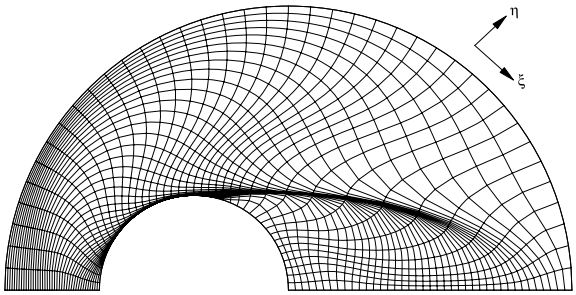

(D1) RL with $r_\xi = 0$ and $r_\eta = 0$.

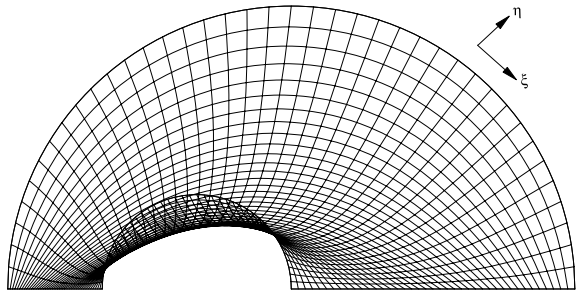

(D2) Conformal mapping.

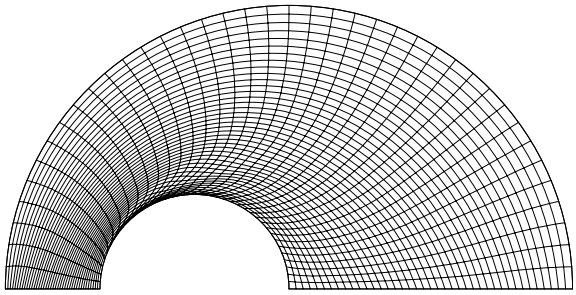

(D3) RL with contribution factors.

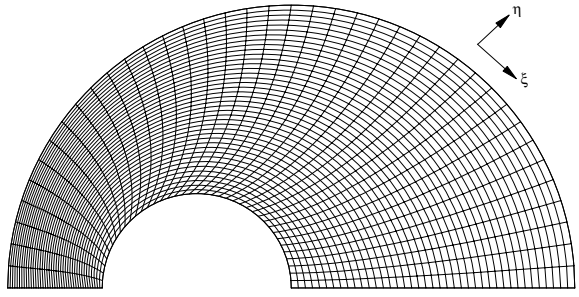

(D4) RL with $r_\xi = 0.5$ and $r_\eta = 0.5$.

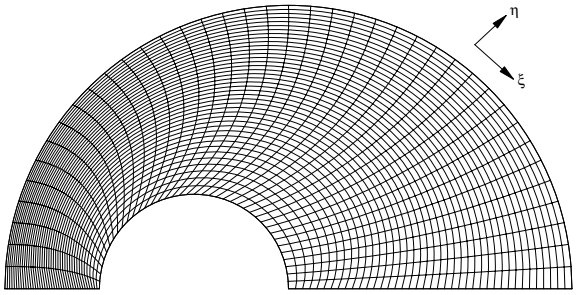

(D5) RL with $r_\xi = 1$ and $r_\eta = 1$.

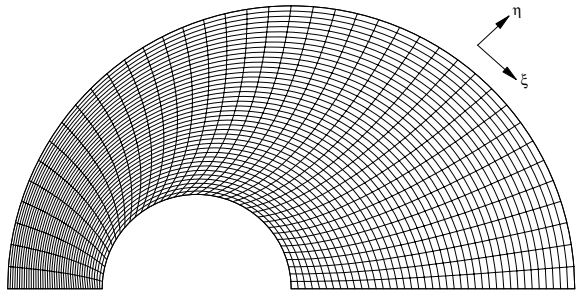

(D6) RL with $r_\xi = 0$ and $r_\eta = 1$.

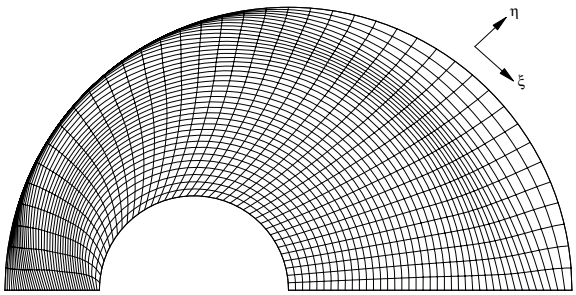

(D7) RL with $r_\xi = 1$ and $r_\eta = 0$.

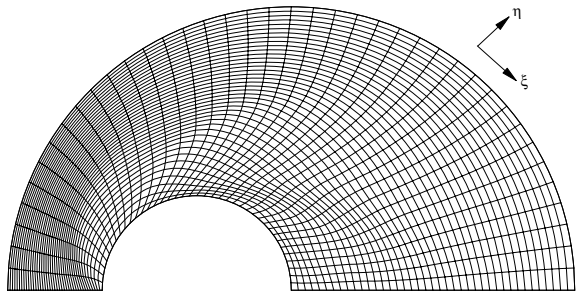

(D8) RL with r_ξ and r_η evaluated by Eq. (15).

Fig. 5. Meshes in domain D.

6. Examples

Two symmetric domains (A and B) and two asymmetric domains (C and D) commonly used in the literatures [1,2,4–6,8,14] are selected to test and illustrate the proposed method. They are defined as follows:

(1) Symmetric domain A (with concave boundary) is bounded by $x = 0$, $x = 1$, $y = 0$, and $y = 0.75 + 0.25\sin(\pi(0.5 + 2x))$.
(2) Symmetric domain B is a unit square with one half-circle on each side.
(3) Asymmetric domain C is bounded by $x = 0$, $y = 0$, $y = 1$, and $x = \frac{1}{2} + \frac{1}{6}\cos(\pi y)$.
(4) Asymmetric domain D is bounded by two-half circles and x axis. The radius of the small circle is one-third of that of the big one.

The proposed method will be compared with the original RL, the conformal mapping, the RL with contribution factors proposed by Zhang et al. [14] using the above domains. The mesh quality is evaluated quantitatively by the standard academic criterions, such as maximum deviation orthogonality (MDO), averaged deviation from orthogonality (ADO), maximum grid aspect ratio (MAR), and averaged grid aspect ratio (AAR). ADO and MDO are used to measure the orthogonality, while AAR and MAR measure the global smoothness. In the present study, the local smoothness is measured by maximum

Table 2
Evaluation of meshes in domains C and D

Domain	Case	Size	ADO	MDO	AAR	MAR	AVS	MVS	r_ξ	r_η	α
C	C1	41×41	0.37	1.11	3.98	46.1	1.1	1.5	0	0	–
	C2	41×41	2.33	6.32	2.17	5.11	1.01	1.17	–	–	–
	C3	41×41	1.98	3.42	2.25	3.75	1.02	1.09	–	–	0.2
	C4	41×41	2.26	3.16	2.19	3.68	1.01	1.02	0.5	0.5	–
	C5	41×41	2.23	5.27	2.18	3.66	1.01	1.02	1	1	–
	C6	41×41	2.09	4.43	2.57	21.38	1.03	1.32	0	1	–
	C7	41×41	2.29	3.40	2.18	3.30	1.01	1.01	1	0	–
	C8	41×41	1.97	2.86	2.28	4.02	1.02	1.08	–	–	–
D	D1	41×41	0.62	3.70	147	5373	1.25	3.56	0	0	–
	D2	41×41	7.2	14.48	3.04	64.5	1.09	3.06	–	–	–
	D3	41×41	3.22	13.2	3.06	8.36	1.05	1.42	–	–	0.6
	D4	41×41	3.58	11.25	3.53	10.56	1.01	1.13	0.5	0.5	–
	D5	41×41	3.79	11.6	3.40	10.15	1.01	1.04	1	1	–
	D6	41×41	3.68	11.84	3.40	9.75	1.01	1.08	0	1	–
	D7	41×41	2.84	9.95	658.2	55,479	1.14	2.71	1	0	–
	D8	41×41	2.96	10.67	3.97	11.14	1.04	1.49	–	–	–

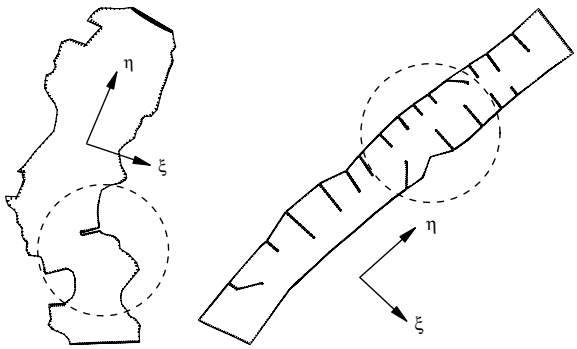

Fig. 6. Layout of domains E and F.

variation of grid sizes (MVS) and averaged variation of grid sizes (AVS). These six indicators are defined as follows:

$$\mathrm{MDO} = \max(\theta_{i,j}) \tag{18a}$$

$$\mathrm{ADO} = \frac{1}{(N_i-2)}\frac{1}{(N_j-2)}\sum_{2}^{N_i-1}\sum_{2}^{N_j-1}\theta_{i,j} \tag{18b}$$

$$\mathrm{MAR} = \max\left[\max\left(f_{i,j},\frac{1}{f_{i,j}}\right)\right] \tag{19a}$$

$$\mathrm{AAR} = \frac{1}{(N_i-2)}\frac{1}{(N_j-2)}\sum_{2}^{N_i-1}\sum_{2}^{N_j-1}\max\left(f_{i,j},\frac{1}{f_{i,j}}\right) \tag{19b}$$

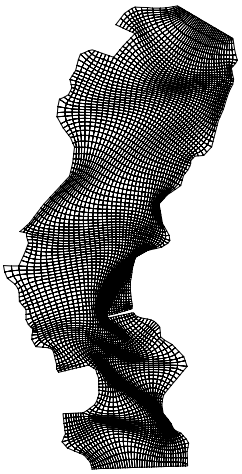

(E1) RL with $r_\xi = 0$ and $r_\eta = 0$.

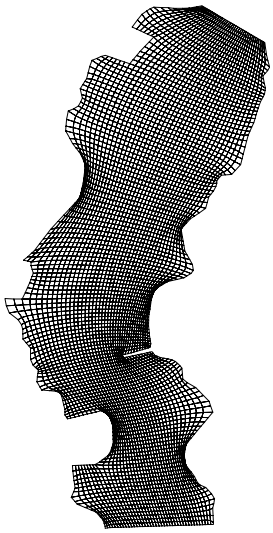

(E2) Conformal mapping.

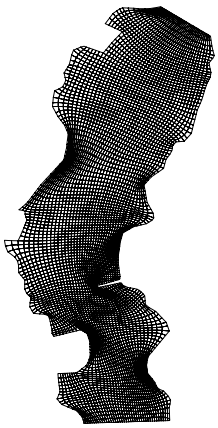

(E3) RL with contribution factors.

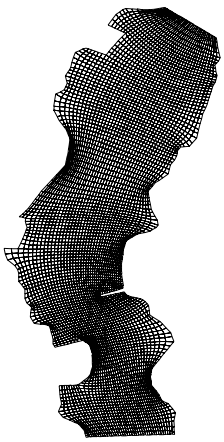

(E4) RL with $r_\xi = 0.5$ and $r_\eta = 0.5$.

Fig. 7. Meshes in domain E (Global).

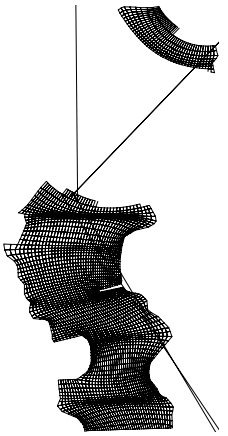

(E8) RL with r [illegible] ted by Eq. (15).

Fig. 7 (*continued*)

$$\mathrm{MVS} = \max\{\max[(S_\xi)_{i,j}, (S_\eta)_{i,j}]\} \tag{20a}$$

$$\mathrm{AVS} = \frac{1}{(N_i - 2)} \frac{1}{(N_j - 2)} \sum_{2}^{N_i - 1} \sum_{2}^{N_j - 1} \max[(S_\xi)_{i,j}, (S_\eta)_{i,j}] \tag{20b}$$

where N_i and N_j are the maximum number of mesh lines in ξ and η directio[illegible]vely; θ is defined as

$$\theta_{i,j} = \left| \arccos\left(\frac{g_{12}}{h_\xi h_\eta}\right)_{i,j} - 90 \right| \tag{21}$$

And, S_ξ and S_η, the variation of grid sizes in ξ and η directions, are defined [illegible]llowing equation:

$$(S_\xi)_{i,j} = \max\left[\frac{(h_\xi)_{i+1/2,j}}{(h_\xi)_{i-1/2,j}}, \frac{(h_\xi)_{i-1/2,j}}{(h_\xi)_{i+1/2,j}}\right] \tag{22a}$$

$$(S_\eta)_{i,j} = \max\left[\frac{(h_\eta)_{i,j+1/2}}{(h_\eta)_{i,j-1/2}}, \frac{(h_\eta)_{i,j-1/2}}{(h_\eta)_{i,j+1/2}}\right] \tag{22b}$$

For all examples, the initial meshes with uniform nodal distribution along the four boundaries, namely, top boundary, bottom boundary, left boundary, and right boundary, were generated by the algebraic method. And, the Dirichlet boundary condition is applied in all boundaries. In the above domains, the ξ direction is from left to right, while the η direction is from bottom to top.

6.1. Sensitivity analysis

Domain D is used to study the effects of r_ξ and r_η on the mesh quality. For simplification purpose, these two parameters are assumed to be equal. Different values of these two parameters ranging from 0.01 to 0.9 were used for mesh generation in this domain.

Fig. 1 illustrates the relationships between these two parameters (r_ξ and r_η) and the indicators (ADO, MDO, AAR, MAR, AVS and MVS) of the mesh quality. As expected, with r_ξ and r_η increasing, ADO and MDO increase, and AAR, MAR, AVS, and MVS decrease. Because the increase of r_ξ and r_η means more deviation from the original RL, it leads to a less orthogonal but smoother mesh.

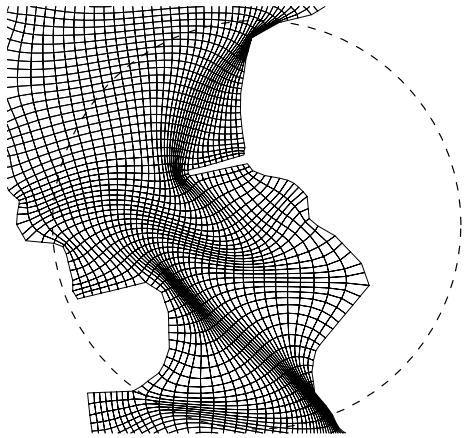

(E1) RL with $r_\xi = 0$ and $r_\eta = 0$.

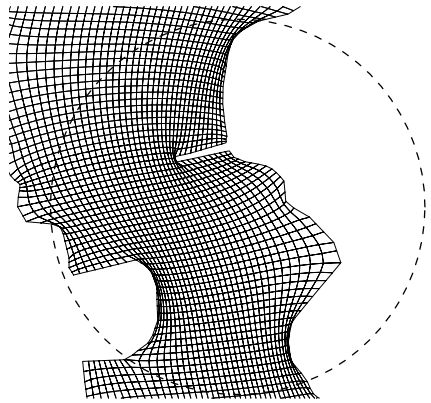

(E2) Conformal mapping.

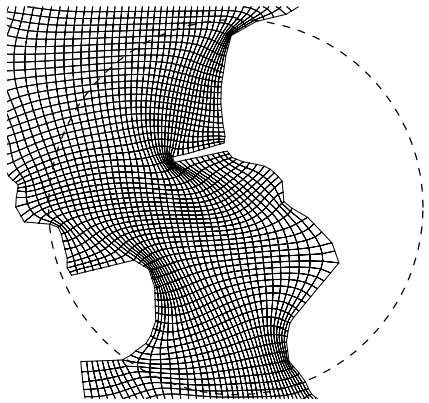

(E3) RL with contribution factors.

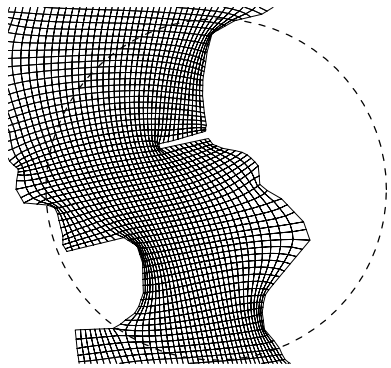

(E4) RL with $r_\xi = 0.5$ and $r_\eta = 0.5$.

Fig. 8. Meshes in domain E (local).

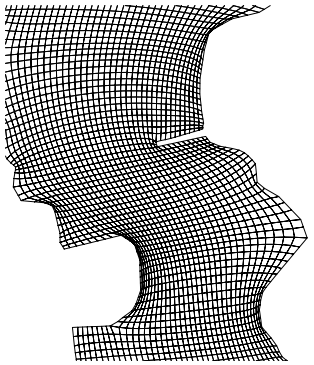

Fig. 8 (*continued*)

A strong variation region of the mesh quality can be identified – r_ξ, $r_\eta \in [0, 0.1]$. The mesh quality changes rapidly within this region and mildly beyond it.

6.2. Symmetric domains

Meshes in domains A and B produced by different methods are illustrated in Figs. 2 and 3, respectively. The quality of final meshes in these two domains is summarized in Table 1.

The conformal mapping generated the folded meshes at the concave boundary of domain A (case A2) and at the four corners of domain B (case B2), while the original RL without controls on distortion function ($r_\xi = 0$ and $r_\eta = 0$) caused the squeezed meshes at the concave boundary of domain A (case A1) and at the center of domain B (case B1), respectively. As stated previously, the folded meshes resulted from the strict local smoothness condition of the conformal mapping, and the squeezed meshes were caused by the strict local orthogonal condition of the RL.

The RL with controls on the scale factors in both directions ($r_\xi = 0.5$ and $r_\eta = 0.5$, and $r_\xi = 1$ and $r_\eta = 1$) relaxed the local orthogonal condition significantly and generated much smoother meshes than the original RL for both domains. However, with the full controls ($r_\xi = 1$ and $r_\eta = 1$), too much smoothness was produced, and the folded meshes occurred in both domains (cases A5 and B5). With less controls ($r_\xi = 0.5$ and $r_\eta = 0.5$), this problem was resolved in domain A (case A4) and alleviated in domain B (case B4).

The controls on the scale factor in only one direction can only improve smoothness in the corresponding direction. For domain A, the RL with controls in η direction ($r_\xi = 0$ and $r_\eta = 1$) resolved the squeezed meshes at the concave boundary but caused mesh lines to be contracted at the left and right boundaries (case A6), and the RL with controls in ξ direction ($r_\xi = 1$ and $r_\eta = 0$) produced even worse mesh with

mesh overlapping at the concave boundary (case A7) . For domain B, the RL with controls in one direction resulted in the squeezed meshes at the center in the other direction without controls (cases B6 and B7).

The RL with automatic controls on the local balance of the orthogonality and the smoothness (r_ξ and r_η evaluated by Eq. (15)) and the RL with contribution factors have similar performances in domain A. Although the latter is better in orthogonality (case A3), the former produced the mesh with best overall quality for domain A (case A8). In domain B, the former failed to generate a mesh without folding due to the four singularities (case B8), but the latter succeeded (case B3).

6.3. Asymmetric domains

Meshes in domains C and D are displayed in Figs. 4 and 5, and Table 2 lists the evaluation report of mesh quality. As can be seen, serious mesh distortions and overlapping occurred in both domains when using the

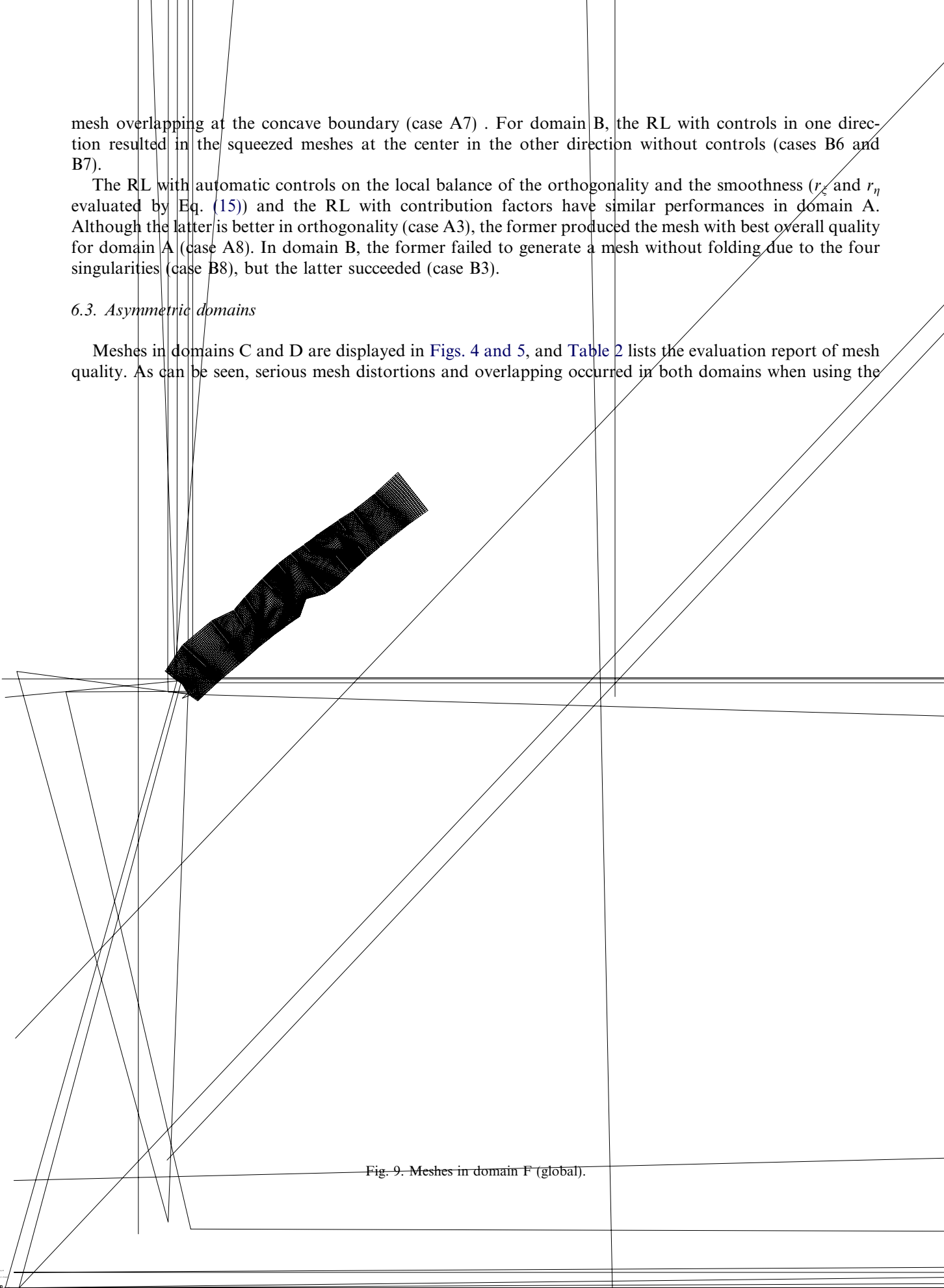

Fig. 9. Meshes in domain F (global).

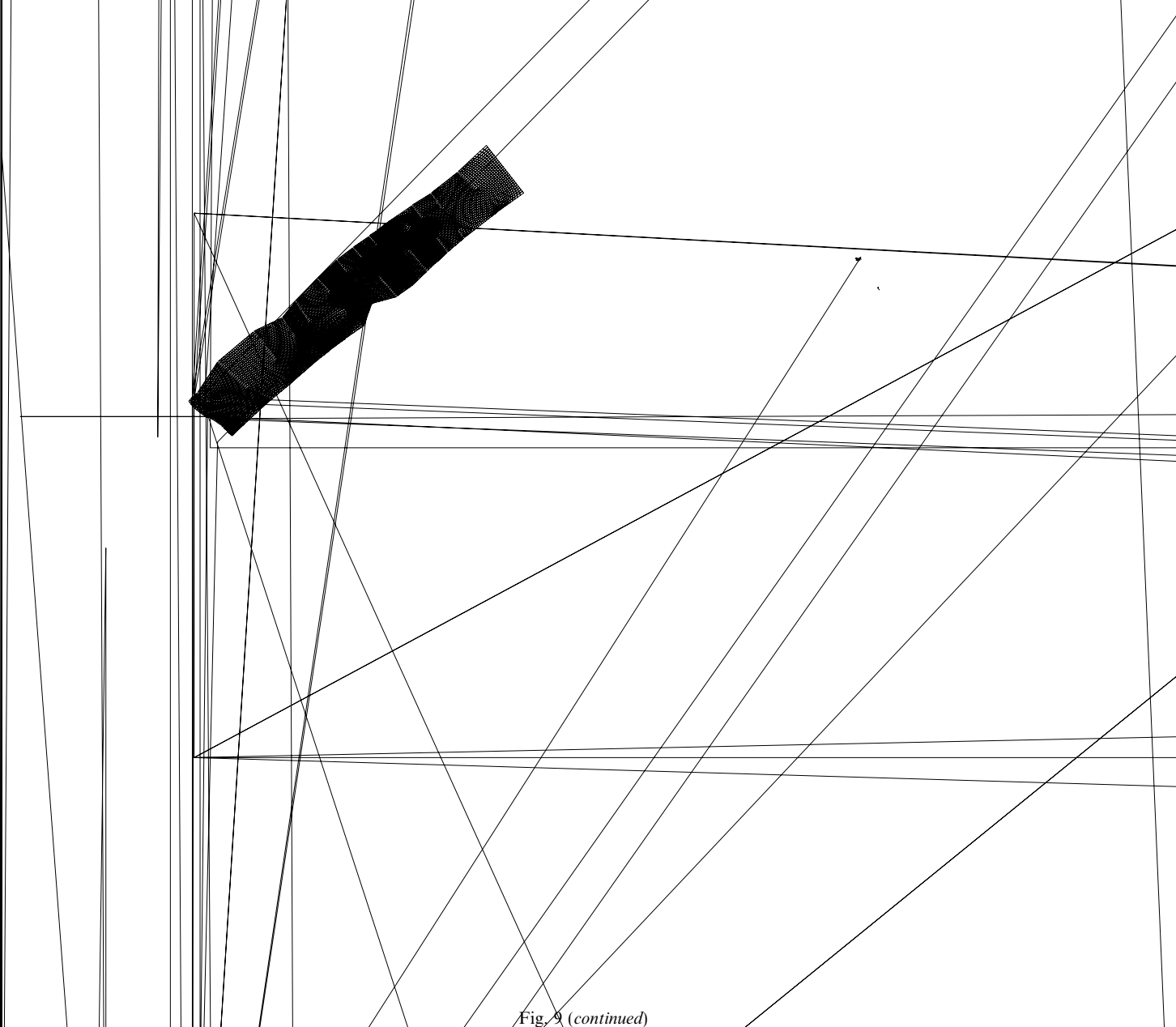

Fig. 9 (*continued*)

original RL (cases C1 and D1), although the best orthogonal meshes were obtained. The conformal mapping failed to generate non-folded mesh in domain D (case D2).

In both domains, the RL with contribution factors, the RL with controls on the scale factors in both directions ($r_\xi = 0.5$ and $r_\eta = 0.5$, and $r_\xi = 1$ and $r_\eta = 1$) and the RL with r_ξ and r_η evaluated by Eq. (15) successfully removed the skewed and squeezed meshes. The RL with r_ξ and r_η evaluated by Eq. (15) (cases C8 and D8) produced better meshes both in orthogonality and smoothness than the others (cases C3, C4, C5, D3, D4, and D5).

The fixed nodal distribution along the right curved boundary of domain C in η direction and the two circular boundaries of domain D in ξ direction resulted in highly distorted meshes when using the original RL. The RL with controls in the corresponding direction (cases C7 and D6) enforces the smoothness in that direction and hence generated smooth meshes without distortions and overlapping in both domains. Without controls in the corresponding direction (cases C6 and D7) caused the mesh lines contract to the right boundary of domain C and the top boundary of domain D, respectively.

7. Applications

To further challenge the proposed method, two natural river channels (domains E and F) are selected for mesh generation. The layouts of the selected channels are displayed in Fig. 6. In addition to the irregular boundaries, there are one spur dike in domain E and 19 spur dikes in domain F, which makes the orthogonal mesh generation a quite difficult task. Since the channel boundaries are very complex, the application of the sliding boundary conditions becomes difficult. Therefore, the Dirichlet boundary conditions were used for all boundaries in both domains. The initial meshes with non-uniform nodal distribution along the boundaries were created by the algebraic method.

Figs. 7 and 9 illustrate the global resulting meshes of these two domains, and Figs. 8 and 10 display the local meshes in the selected circled zones. The evaluation report is summarized in Table 3. Not surprisingly, the original RL failed in both domains in which highly distorted regions existed (cases E1 and F1). As for the conformal mapping, although the mesh smoothness was globally improved, the folded meshes occurred in the circled zones of both domains (cases E2 and F2).

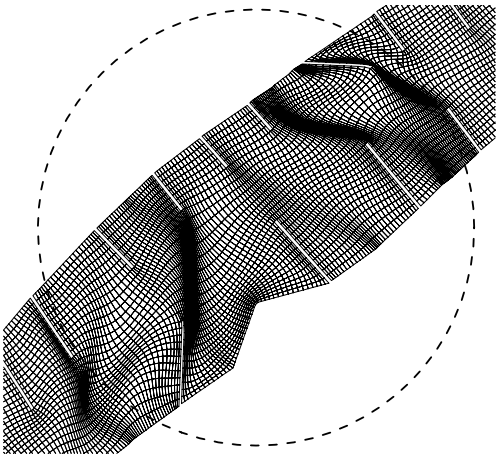

(F1) RL with $r_\xi = 0$ and $r_\eta = 0$.

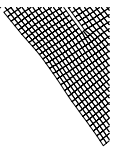

Fig. 10. Meshes in domain F (local).

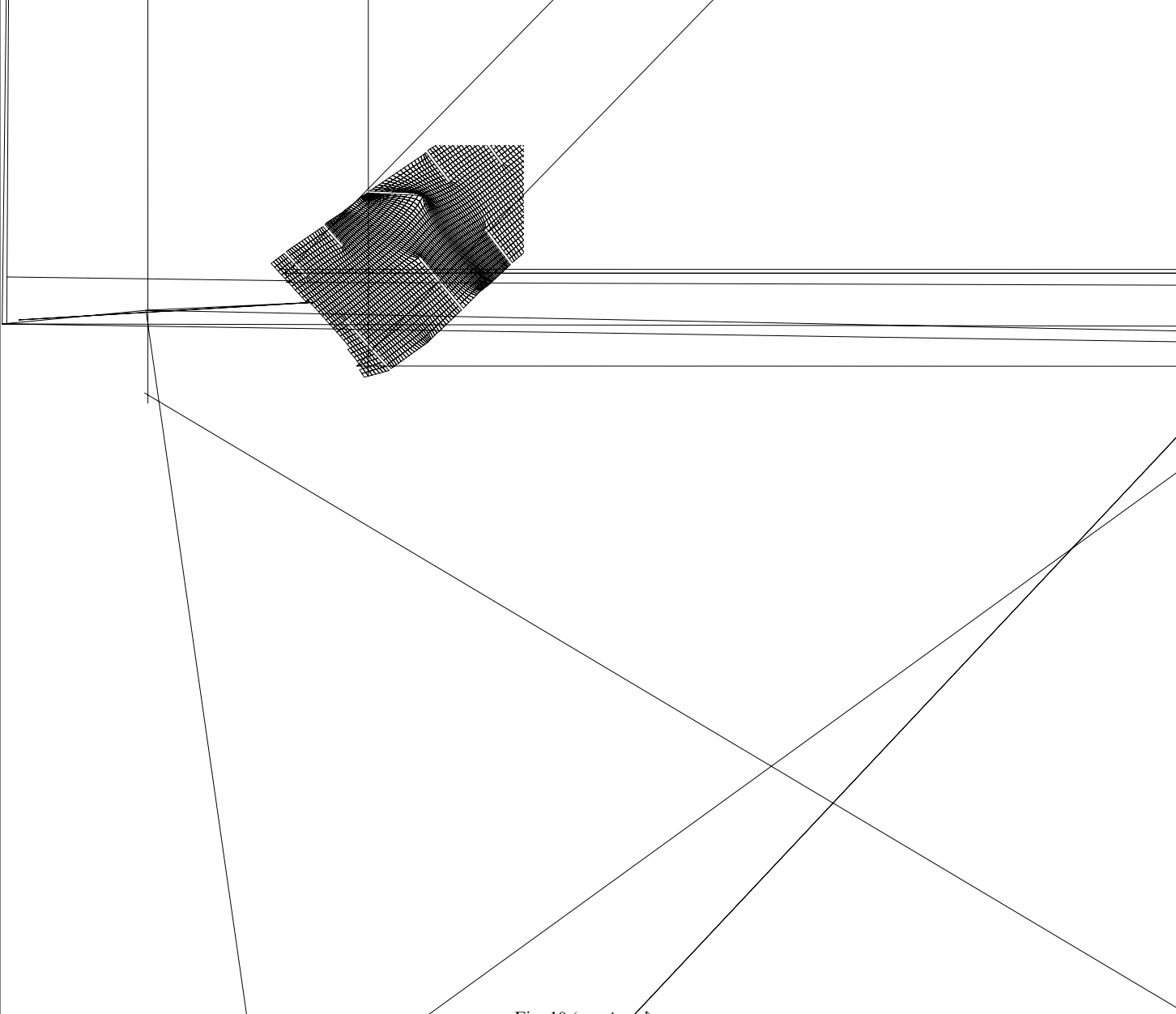

Fig. 10 (*continued*)

Using the RL with controls in only one direction, the mesh distortion was removed from both domains. However, the RL with controls in η direction ($r_\xi = 0$ and $r_\eta = 1$) caused the mesh lines contracted to the tip of the dike of domain E in ξ direction (case E6). It generated smooth mesh but with little mesh folding at the tip of the oblique dikes in domain F (case F6). As for the RL with controls in ξ direction ($r_\xi = 1$ and $r_\eta = 0$), it resulted in the squeezed meshes at the center of domain E (case E7) and at the oblique dikes of domain F (case F7).

In domain E, the RL with contribution factors, the RL with controls on two directions ($r_\xi = 0.5$ and $r_\eta = 0.5$, and $r_\xi = 1$ and $r_\eta = 1$) and the RL with r_ξ and r_η evaluated by Eq. (15) succeeded in producing smooth meshes without distortion, overlapping and folding (cases E3, E4, E5 and E8). In domain F, the RL with controls on both directions generated the folded meshes at the tips of the oblique dikes (cases F4 and F5), while the RL with contribution factors and the RL with r_ξ and r_η evaluated by Eq. (15) successfully resolved this problem (cases F3 and F8). In both domains, the meshes with best overall quality (cases E8 and F8) were obtained from the RL with controls on the local balance of the orthogonality and the smoothness.

Table 3
Evaluation of meshes in domains E and F

Domain	Case	Size	ADO	MDO	AAR	MAR	AVS	MVS	r_ξ	r_η	α
E	E1	41×137	0.29	3.90	2.30	65.1	1.11	2.02	0	0	–
	E2	41×137	2.69	14.46	1.37	12.8	1.05	2.37	–	–	–
	E3	41×137	1.48	7.76	1.58	9.3	1.07	1.88	–	–	0.24
	E4	41×137	2.24	13.56	1.40	5.90	1.06	1.70	0.5	0.5	–
	E5	41×137	2.72	14.27	1.42	8.0	1.06	2.19	1	1	–
	E6	41×137	1.52	10.98	2.48	263.7	1.14	3.31	0	1	–
	E7	41×137	2.40	14.40	1.72	11.62	1.11	8.54	1	0	–
	E8	41×137	1.70	12.0	1.54	5.09	1.07	2.0	–	–	–
F	F1	30×374	0.43	5.70	2.81	161.4	1.10	2.45	0	0	–
	F2	30×374	2.55	14.48	1.78	8.25	1.02	2.18	–	–	–
	F3	30×374	2.08	14.37	1.86	10.13	1.03	1.60	–	–	0.52
	F4	30×374	2.27	14.46	1.81	6.60	1.02	1.60	0.5	0.5	–
	F5	30×374	2.53	14.44	1.78	6.74	1.02	1.89	1	1	–
	F6	30×374	2.33	14.47	1.79	7.14	1.05	1.88	0	1	–
	F7	30×374	2.02	14.14	3.31	468.4	1.06	3.72	1	0	–
	F8	30×374	1.82	14.46	1.90	9.55	1.05	1.85	–	–	–

8. Conclusions

In computational fluids dynamics (CFD), practical fluids flows are often associated with complex domains, in which the absolutely orthogonal mesh generation becomes difficult or even impossible when using the classical generation systems – the RL system and the conformal mapping. In the RL system, the distortion function is controlled only by the local orthogonal conditions, which results in the unpredictable distribution of the mesh density. In the conformal mapping system, the distortion function is enforced with a constant value. To improve their disadvantages, a new method to control the distortion function has been developed.

In the proposed method, both the averaged scale factors and the local scale factors are used to evaluate the distortion function. It therefore takes into account the effects of both the local orthogonal condition characterized by the local scale factors, and the local smoothness conditions (the geometry and the mesh size) characterized by the averaged scale factors. In this way, both the strict local orthogonal condition of the RL system and the strict local smoothness condition of the conformal mapping system are relaxed and consequently only nearly orthogonal meshes but with adequate smoothness can be obtained.

Two adjustable parameters r_ξ and r_η are used to control the ratio of the local scale factors and the averaged scale factors in ξ and η directions and hence the local balance of the orthogonality and the smoothness. These two parameters can either be user-specified with the constant values through the whole domain or automatically evaluated by the indicators of the local *relative smoothness conditions* which are defined as the ratio of the difference and the sum of the local scale factors and the averaged scale factors. The smoother the mesh is, the smaller these two parameters are, and the smaller the effects of the averaged scale factors on the distortion function will be.

Several benchmark examples are selected to demonstrate and compare the proposed method with the original RL system, the conformal mapping system and the RL with contribution factors proposed by Zhang et al. [14]. The controls on both directions generally improved the global smoothness significantly, but it caused slightly folded meshes in some domains. With controls on only one direction, the smoothness in the corresponding direction can be improved. The automatic controls on the local balance of the orthogonality and the smoothness produced meshes with the best overall quality. For most cases, the RL with contribution factors have similar performances to the RL with automatic controls on the distortion fucntion. All methods except the RL with contribution factors failed to generate a good mesh without distortions, overlapping and folding in domain B due to the four singularity corners. The sensitivity analysis in domain D shows that the parameters r_ξ and r_η have significant effects on the mesh quality in the range of $[0, 0.1]$, and out of this range these two parameters have much less influence.

The proposed method was also applied to two natural channels with complex geometries. It has been shown that the proposed method is capable of generating nearly orthogonal meshes with a good balance of the orthogonality and the smoothness in these two geometrically complex domains where the original RL system and the conformal mapping system have failed.

Acknowledgements

This work is a result of research sponsored by the USDA Agriculture Research Service under Specific Research Agreement No. 58-6408-2-0062 (monitored by the USDA-ARS National Sedimentation Laboratory) and The University of Mississippi.

References

[1] V. Akcelik, B. Jaramaz, O. Ghattas, Nearly orthogonal two-dimensional grid generation with aspect ratio control, J. Comput. Phys. 171 (2001) 805–821.
[2] A. Allievi, S.M. Calisal, Application of Bubnov–Galerkin formulation to orthogonal grid generation, J. Comput. Phys. 98 (1992) 163–173.
[3] R. Arina, Orthogonal grids with adaptive control, in: J. Hauser, C. Taylor (Eds.), Proceedings of the First International Conference on Numerical Grid Generation in CFD, Pineridge Press, Swansea, 1986.
[4] R. Duraiswami, A. Prosperetti, Orthogonal mapping in two dimensions, J. Comput. Phys. 98 (1992) 254–268.
[5] L. Eça, 2D orthogonal grid generation with boundary point distribution control, J. Comput. Phys. 125 (1996) 440–453.
[6] I.S. Kang, L.G. Leal, Orthogonal grid generation in a 2D domain via the boundary integral technique, J. Comput. Phys. 102 (1992) 78–87.
[7] C.D. Mobley, R.J. Stewart, On the numerical generation of boundary-fitted orthogonal curvilinear coordinate systems, J. Comput. Phys. 34 (1980) 124–135.
[8] H.J. Oh, I.S. Kang, A non-iterative scheme for orthogonal grid generation with control function and specified boundary correspondence on three sides, J. Comput. Phys. 112 (1994) 138–148.
[9] S.B. Pope, The calculation of turbulent recirculating flows in general orthogonal coordinates, J. Comput. Phys. 26 (1978) 197–217.
[10] G. Ryskin, L.G. Leal, Orthogonal mapping, J. Comput. Phys. 50 (1983) 71–100.
[11] P. Tamamidis, D.N. Assanis, Generation of orthogonal grids with control of spacing, J. Comput. Phys. 94 (1991) 437–453.
[12] J.F. Thompson, F.C. Thames, C.W. Mastin, TOMCAT – A code for numerical generation of boundary-fitted curvilinear coordinate system on fields containing any number of arbitrary two-dimensional bodies, J. Comput. Phys. 24 (1977) 274–302.
[13] J.F. Thompson, Z.U.A. Warsi, C.W. Mastin, Numerical Grid Generation: Foundation and Application, North-Holland, New York, 1985.
[14] Y.X. Zhang, Y.F. Jia, Sam S.Y. Wang, 2D nearly orthogonal mesh generation, Int. J. Numer. Methods Fluids 46 (2004) 685–707.